V. MICROWAVE ELECTRONICS

Prof. L. D. Smullin
Prof. H. A. Haus
Prof. A. Bers
Prof. L. J. Chu
P. A. Mandics
R. P. Porter
H. M. Schneider

A. HIGH-PERVEANCE HOLLOW ELECTRON-BEAM STUDY

Direct-current and radiofrequency interaction measurements have been completed on both a cylindrical-cathode and a conical-cathode magnetron injection electron gun. Detailed dc measurements on the cylindrical-cathode gun have been performed previously, and have been described by Poeltinger.[1] The guns described in this report were operated with 1-μsec pulses at voltages up to V_a = 8 kv. All rf interaction measurements were performed at f = 1119 mc. Figure V-1 is a schematic diagram of the beam tester. The first cavity is provided with two coupling loops (not shown) for the

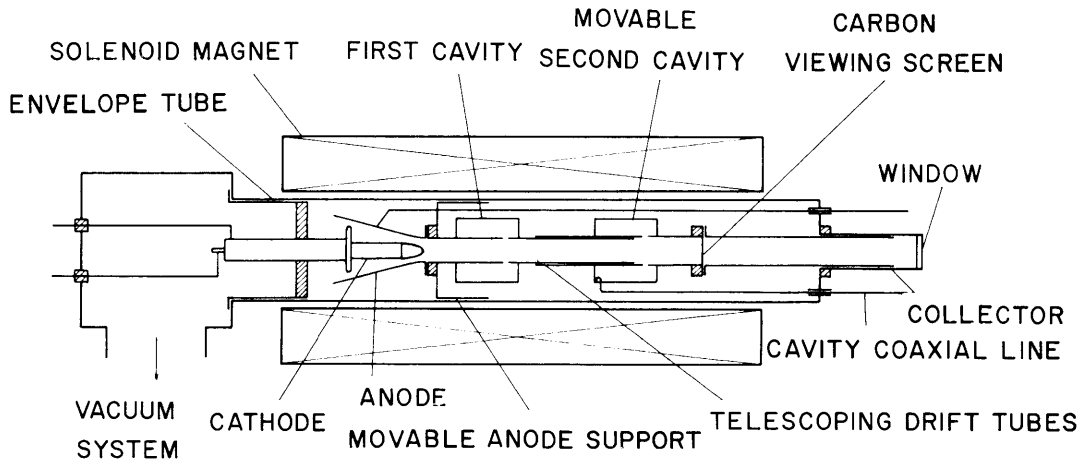

Fig. V-1. Schematic diagram of the beam tester.

measurement of beam loading. Figure V-2 gives the general layout of the cathodes, cavity gaps, and mesh target for viewing the beam cross section.

1. Cylindrical-Cathode Gun

a. Measurement of the Beam Dimensions

The beam dimensions were determined by observing the heating of a carbonized nylon mesh screen that was placed in the path of the beam (see Fig. V-1). Photographs of some typical beam cross sections are shown in Fig. V-3. These are pertinent to the previously measured dc characteristics of a cylindrical-cathode gun.[1]

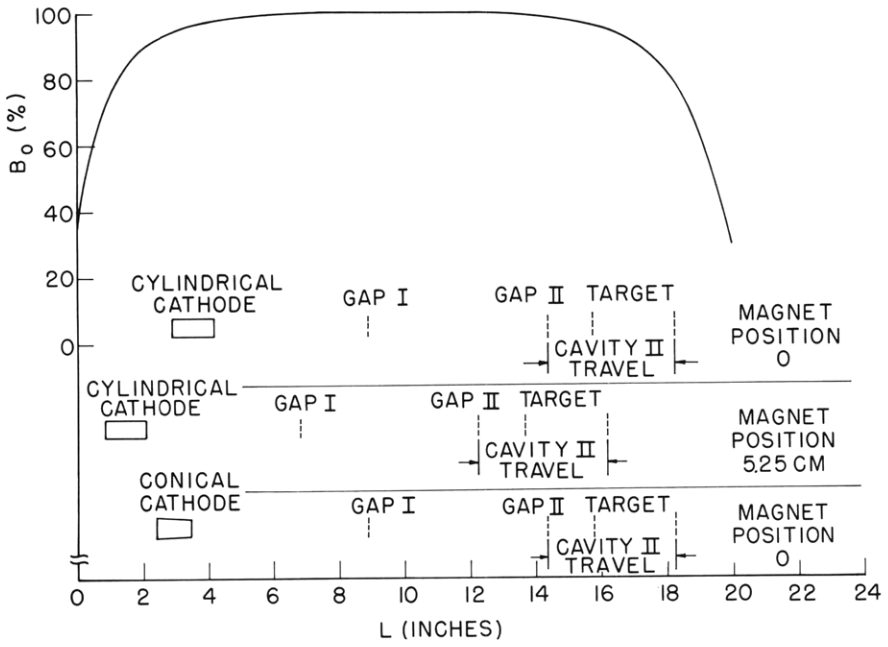

Fig. V-2. Relative magnetic flux density vs length of the magnet.

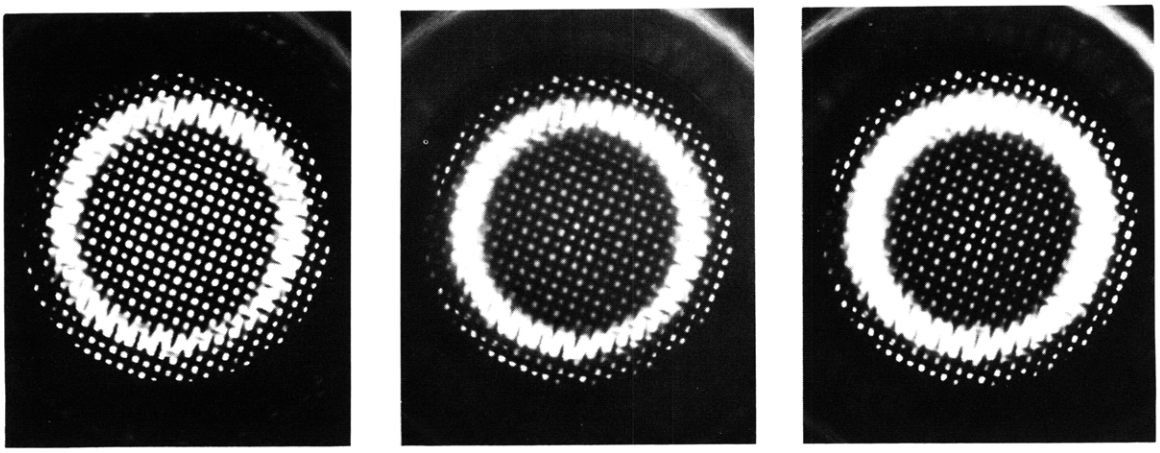

U_o = 6 KV
I_o = 5.2 A
K_o = 11.2 $\mu AV^{-3/2}$
B = 1330 G
a = 0.98 cm
b = 0.81 cm
c = 0.66 cm

U_o = 7 KV
I_o = 6.4 A
K_o = 10.9 $\mu AV^{-3/2}$
B = 1660 G
a = 0.98 cm
b = 0.81 cm
c = 0.65 cm

U_o = 8 KV
I_o = 8.2 A
K_o = 11.5 $\mu AV^{-3/2}$
B = 1590 G
a = 0.98 cm
b = 0.84 cm
c = 0.62 cm

Fig. V-3. Hollow-beam cross sections.

Results of beam cross section measurements for a new gun that was used to take all the rest of the data are summarized in the top of Fig. V-4. The accuracy of the

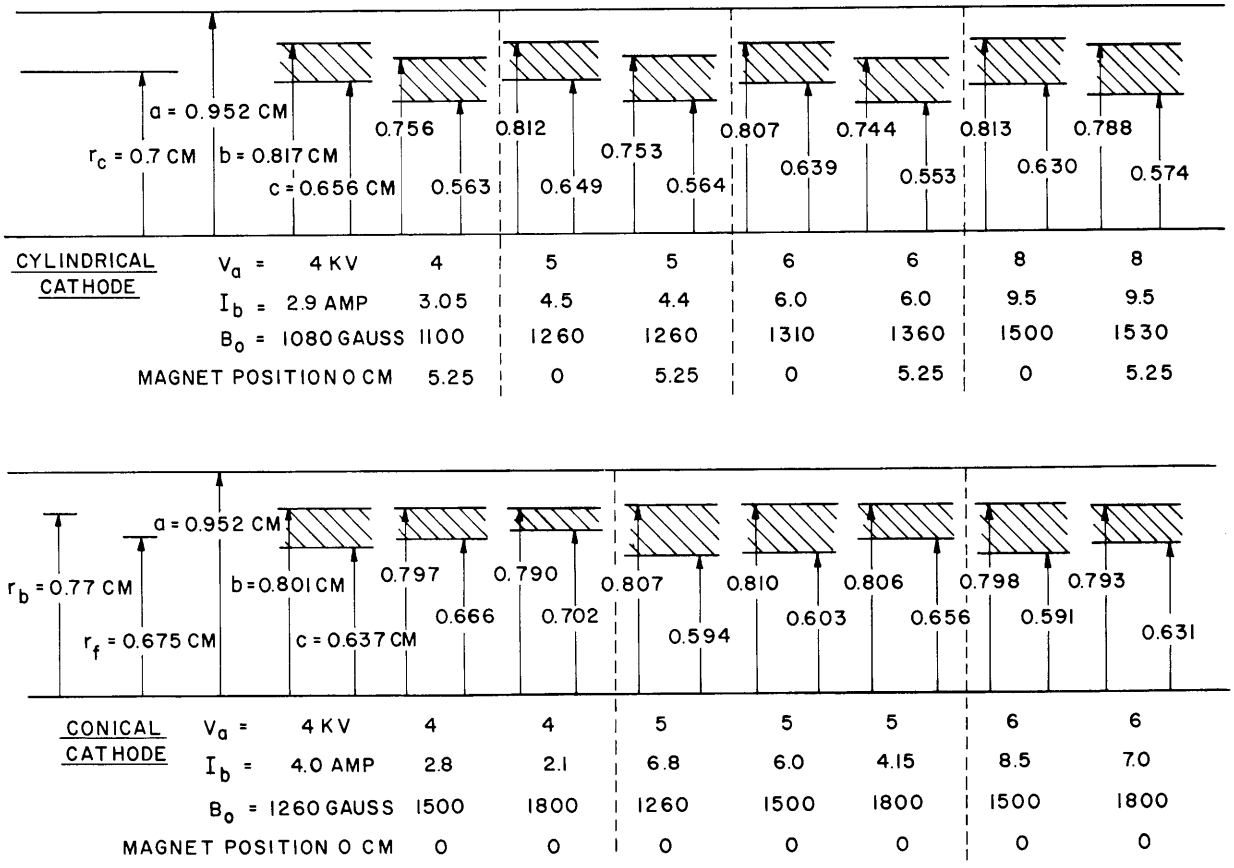

Fig. V-4. Beam dimensions.

dimensions obtained in this way was approximately 20 per cent.

b. Beam Loading

The real part of the electronic admittance G_{el} was measured by using the first cavity as a transmission cavity. The experimental arrangement for these measurements is diagrammed in Fig. V-5. G_{el} was calculated from the measured bandwidth of the cavity with and without the beam. These measurements, as well as the space-charge wavelength and gain measurements, were performed for two different magnet positions as shown in Fig. V-2. The measured and calculated dc parameters for all of the measurements are presented in Table V-1. The results of the beam-loading measurements are listed in Table V-2.

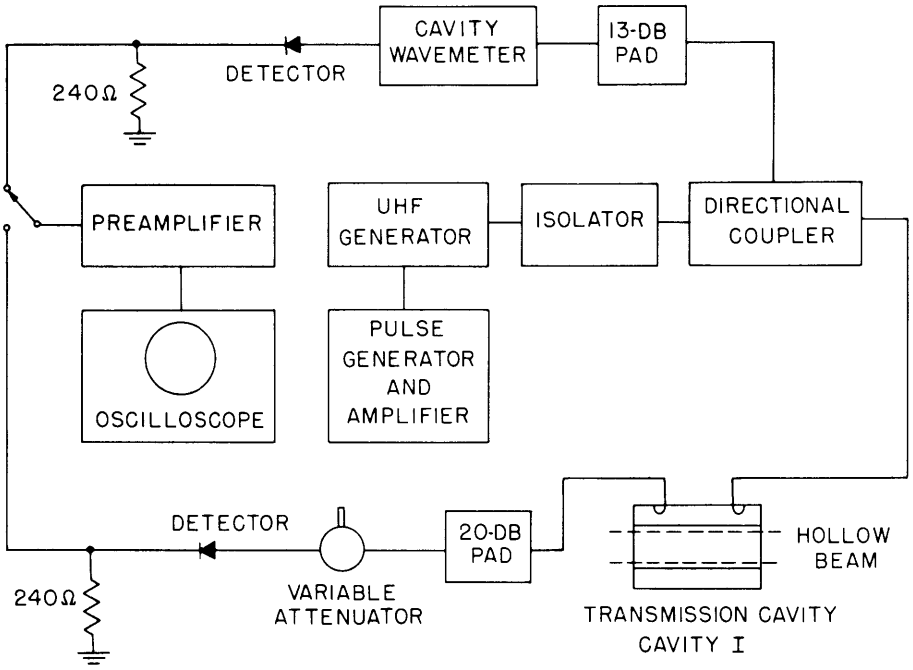

Fig. V-5. Beam-loading measurement.

Table V-1. D-C characteristics of the cylindrical-cathode gun.

Case	V_a (kv)	V_b (kv)	I_b (amp)	B_o (gauss)	Magnet Position (cm)	K (microperv)	f_p (mc)
1	2	1.92	0.8	1030	0	9.0	–
2	2	1.86	0.8	1030	5.25	9.0	–
3	4	3.80	2.9	1080	0	11.4	742
4	4	3.68	3.1	1100	5.25	12.0	743
5	5	4.77	4.5	1260	0	12.7	866
6	5	4.59	4.4	1260	5.25	12.5	854
7	6	5.70	6.0	1310	0	12.9	954
8	6	5.47	6.0	1360	5.25	12.9	960

Table V-2. Beam loading of the cylindrical-cathode gun.

Case	G_{el}			
	Measurement	Calculation		
	$((ohm)^{-1} \times 10^6)$	Kinematic Theory $((ohm)^{-1} \times 10^6)$	Kinematic Theory Thin Beam ($b \approx c$) $((ohm)^{-1} \times 10^6)$	Space-Charge Theory Thin Beam ($b \approx c$) $((ohm)^{-1} \times 10^6)$
1	72.9	–	–	–
2	71.5	–	–	–
3	129	100	104	108
4	149	121	121	124
5	120	129	126	127
6	144	138	143	139
7	–	126	133	135
8	–	164	157	155

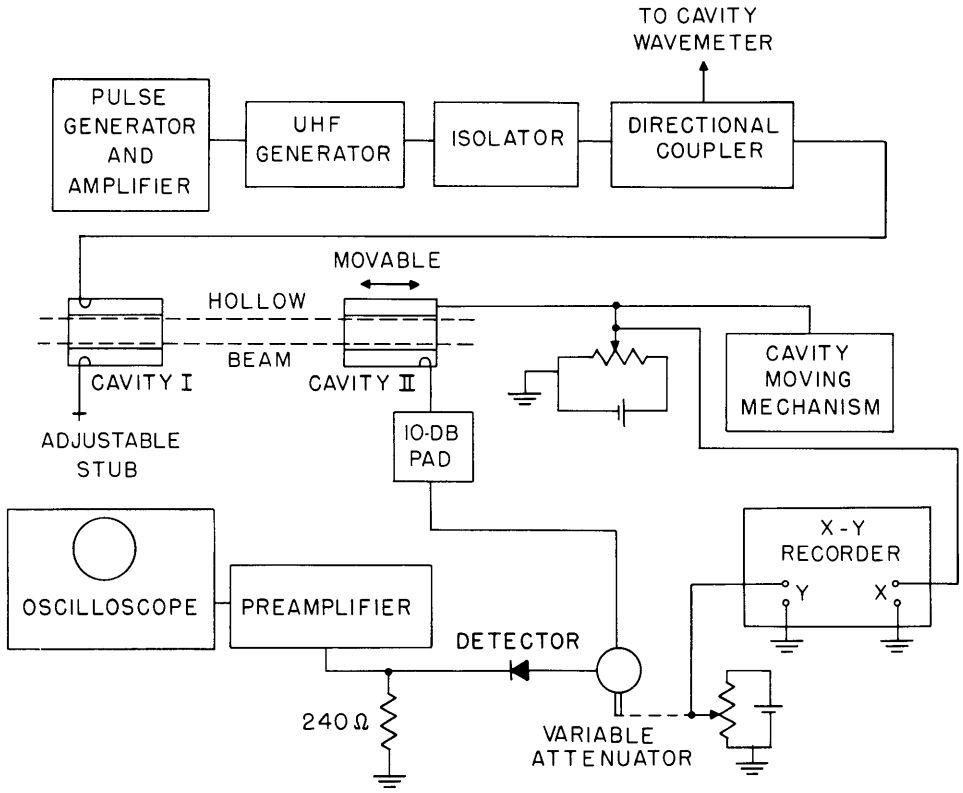

Fig. V-6. Space-charge wavelength, gain and noise measurement.

For purposes of comparison, G_{el} was calculated by using the approximate kinematic[2] and space-charge[3] theories based on a thin-beam assumption (b-c $\ll$c), and also by using the exact kinematic formulation.[2] The calculated values are also tabulated in Table V-2.

c. Space-Charge Wavelength and Gain

The space-charge wavelength and two-cavity gain were measured by using the arrangement illustrated in Fig. V-6. With a constant power input into the first cavity, the second cavity was moved along the beam and the power output from the second cavity was plotted against distance. The resultant curves are plotted in Fig. V-7.

The space-charge wavelength λ_q was calculated by making use of the plasma frequency-reduction factors of Branch and Mihran.[4] The available two-cavity gain was determined from the formulation given by Bers.[3] These theoretical values are compared with the experimental results in Table V-3.

d. Noise

The noise power output from the second cavity was plotted against distance along the beam for four different voltage settings. The circuit used for these measurements

Table V-3. Space-charge wavelength and gain of the cylindrical-cathode gun.

Case	Measurement		Calculation			
	λ_q (cm)	Gain (db)	λ_q (cm)	Gain (db)	M^2	M^2Y_o $((ohm)^{-1}\times 10^3)$
1	17.1	7.8	17.5	–	–	–
2	15.0	6.2	13.8	–	–	–
3	18.2	9.4	19.7	10.5	0.545	1.16
4	11.9	2.6	14.8	4.74	0.458	0.701
5	18.9	10.0	19.5	13.1	0.593	1.45
6	13.3	3.9	15.6	7.4	0.511	0.913
7	19.2	8.5	20.6	13.4	0.627	1.58
8	11.8	4.0	16.4	6.1	0.554	0.92

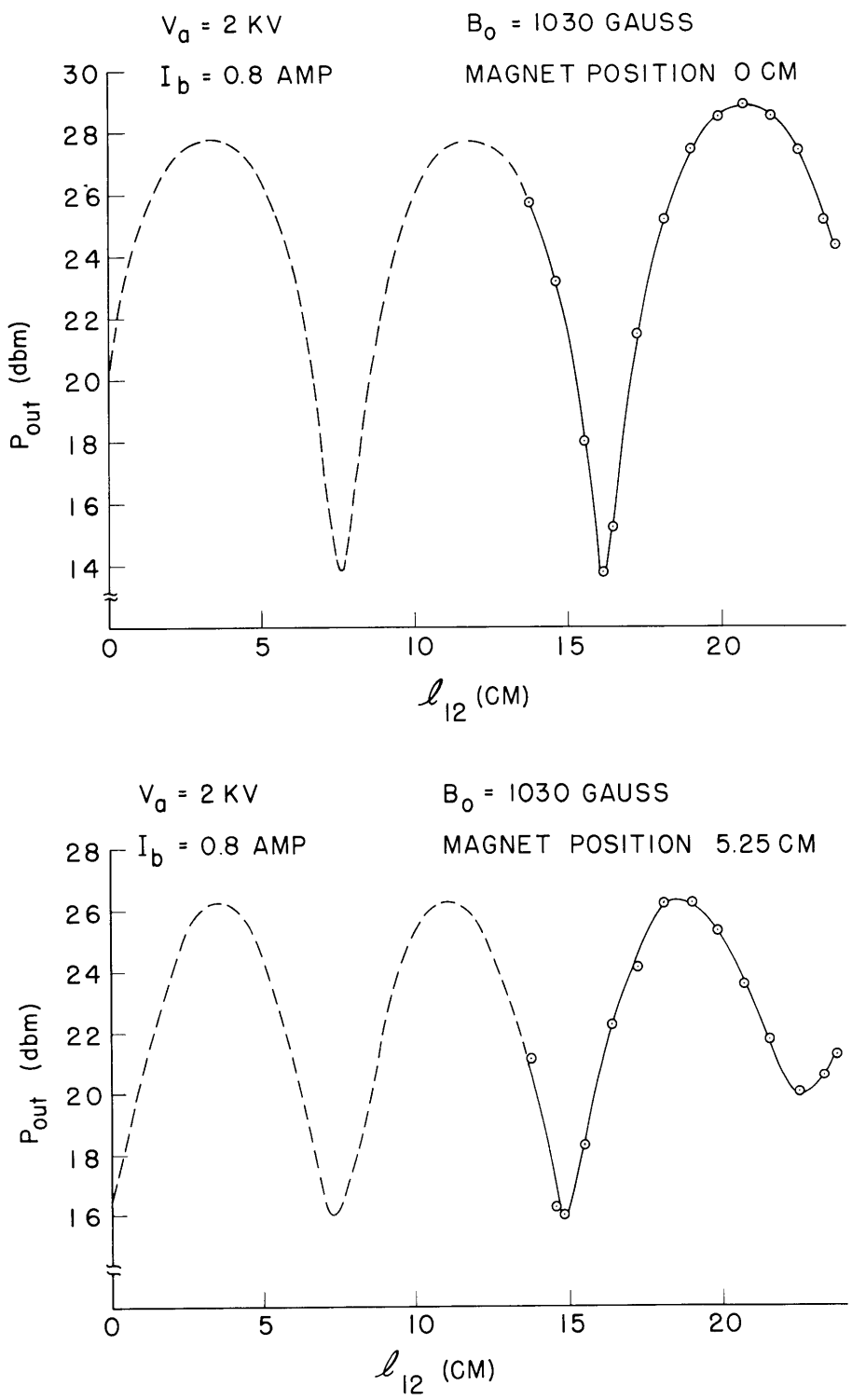

Fig. V-7. Second-cavity power output vs distance between cavity gaps for the cylindrical-cathode gun. (Cavity I, P_{in} = 20 dbm.)

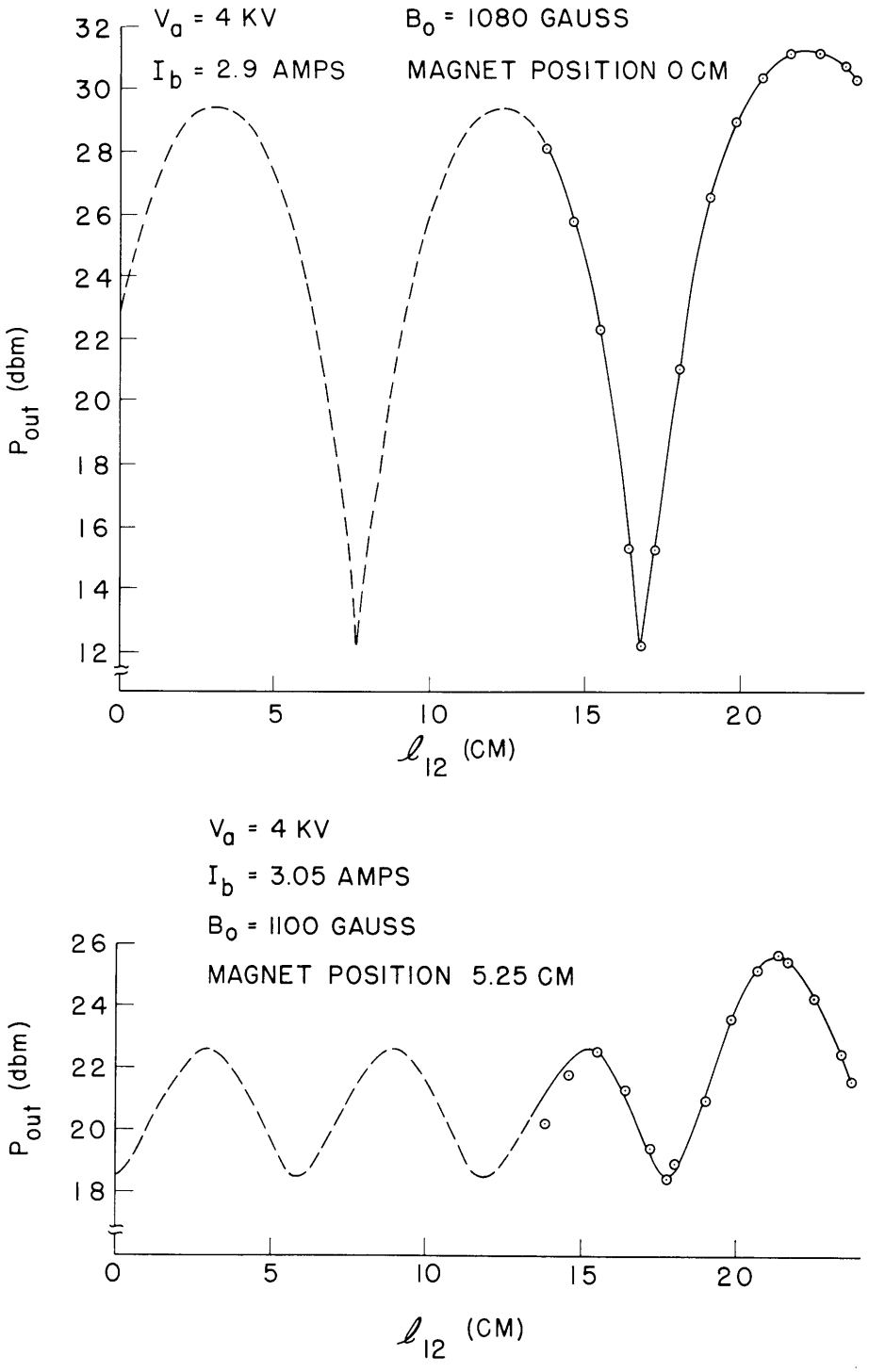

Fig. V-7. (continued).

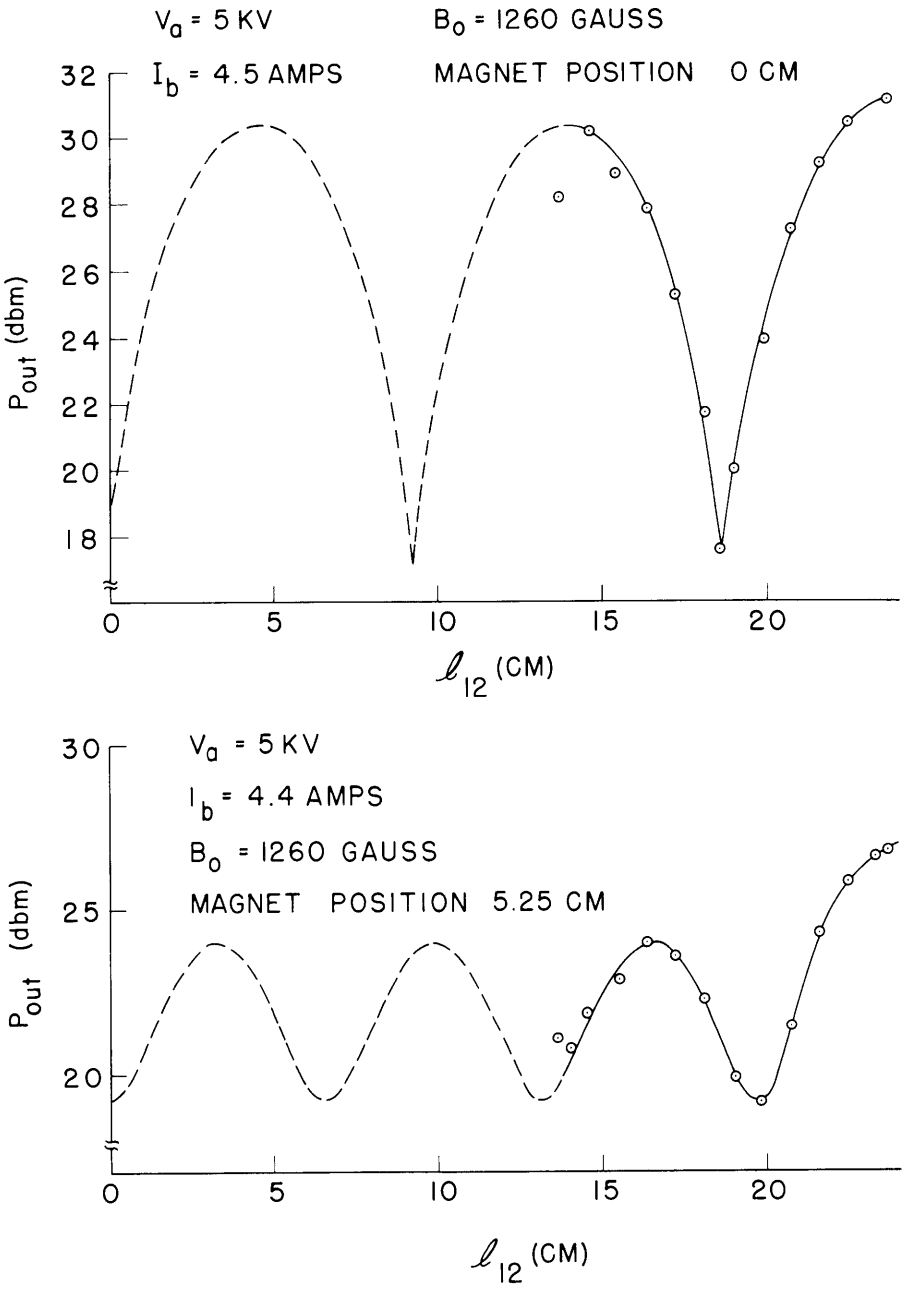

Fig. V-7. (continued).

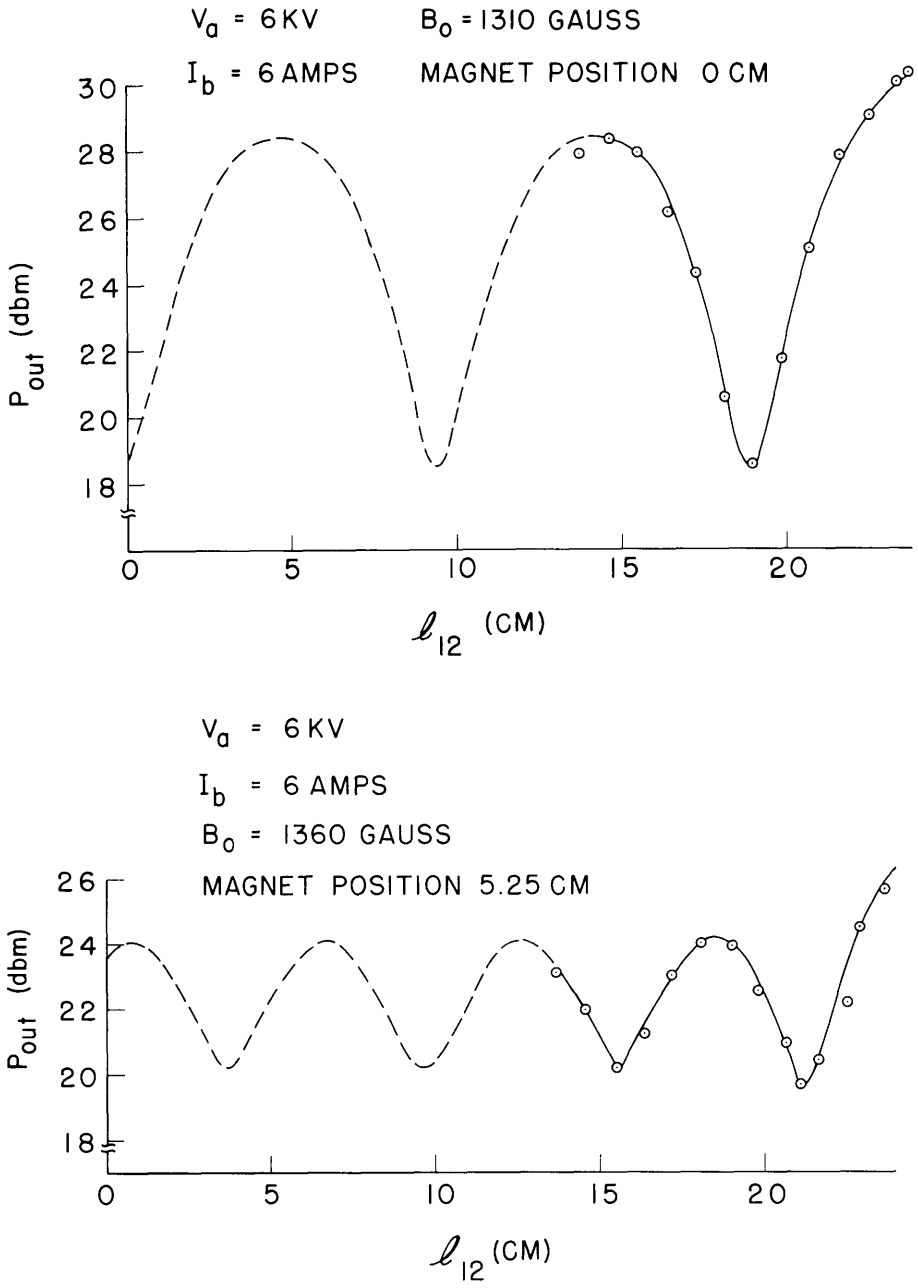

Fig. V-7. (concluded).

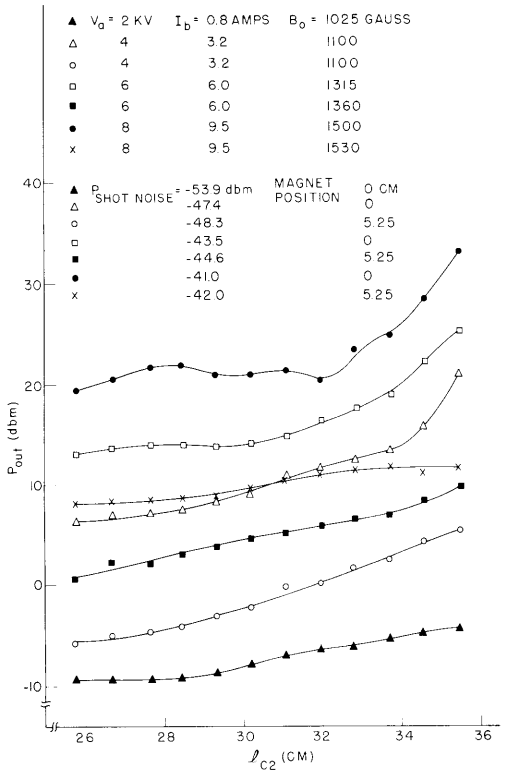

Figure V-8.

Second-cavity noise power output vs distance between cathode and cavity gap for the cylindrical-cathode gun.

was identical to the one shown in Fig. V-6, with the exception that the power input to the first cavity was disconnected. In Fig. V-8 the results of these measurements are presented. It is quite apparent from Fig. V-8 that for a nonuniform magnetic field over

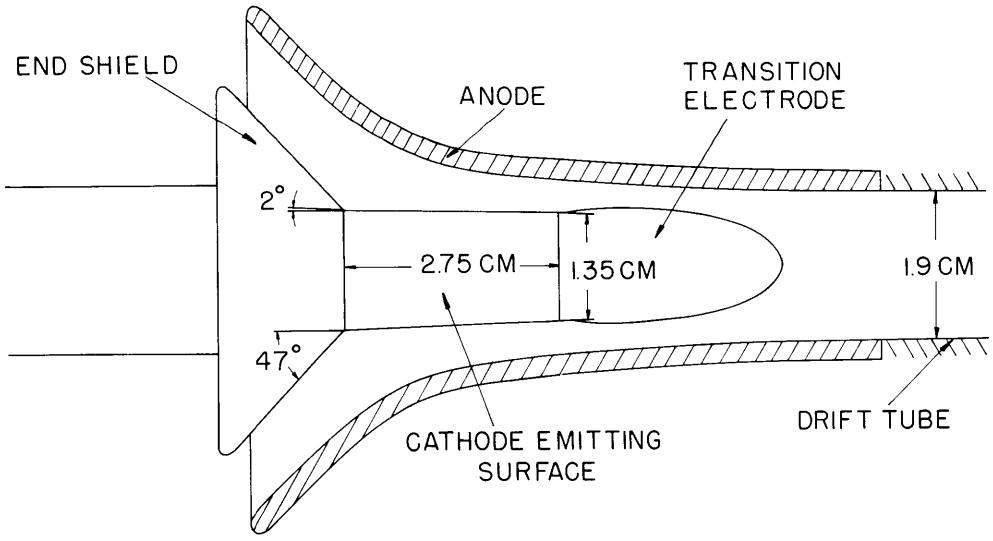

Fig. V-9. Conical-cathode magnetron injection gun.

the cathode corresponding to magnet position 5.25 cm (consult Fig. V-2) the noise output is drastically reduced. It was also observed that the noise output increased for an increase in the magnetic field. For all seven curves the noise output increases along the beam. In one case it increases by as much as 3 db/cm.

2. Conical-Cathode Gun

The design data and computer results for the electrode shapes of this gun have been described in a previous report.[5] After the cylindrical corrections[6] were carried out, the electrodes had the dimensions shown in Fig. V-9.

a. D-C Measurements

The results of the beam-dimension measurements are given at the bottom of Fig. V-4. In general, the beam cross section appeared to be quite symmetric. Beam breakup was observed only for low magnetic fields and high perveance, for example, for V_a = 7 kv, I_b = 10 amps, and magnetic field B_o = 925 gauss. The perveance $K = \frac{I_b}{V_a^{3/2}}$ is plotted against the magnetic field in Fig. V-10. For very high magnetic fields and relatively low voltages, V_a = 2, 3, and 4 kv, the perveance seemed to reach a limiting value of K = 7.5 microperv. On account of magnetic-field limitations, it was not possible to determine whether or not the higher voltage curves would also approach this (or some other) limit.

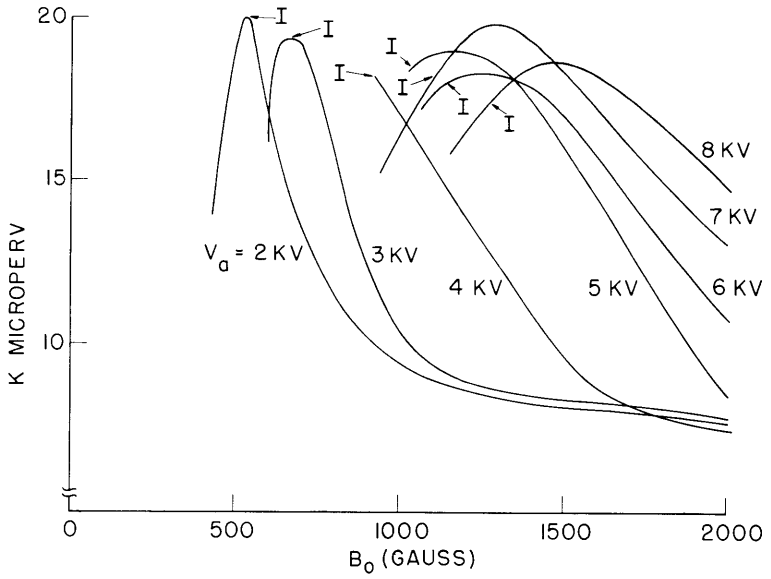

Fig. V-10. Beam perveance vs magnetic field for the conical-cathode gun.

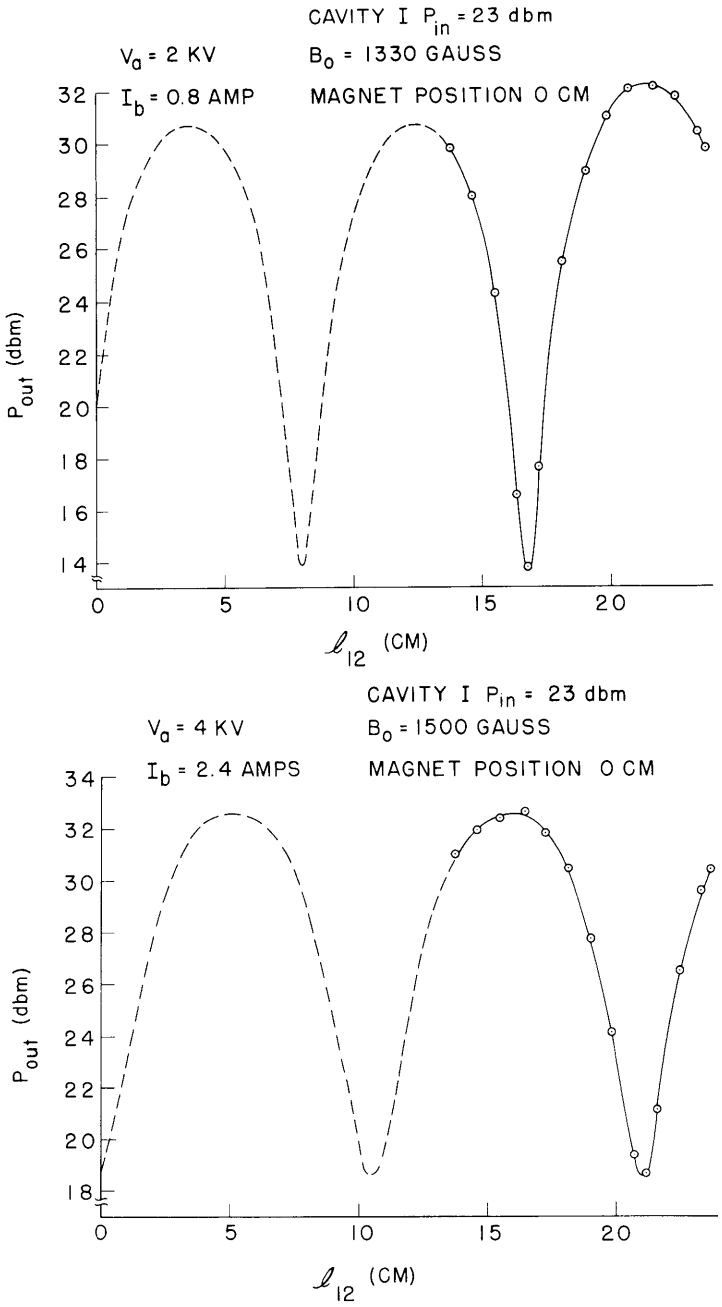

Fig. V-11. Second-cavity power output vs distance between cavity gaps for the conical-cathode gun.

Table V-4. D-C characteristics, space-charge wavelength, and gain of the conical-cathode gun.

Measurement							
V_a (kv)	V_b (kv)	I_b (amp)	B_o (gauss)	Magnet Position (cm)	K (microperv)	λ_q (cm)	Gain (db)
4	3.79	2.4	1500	0	9.5	21.0	9.6

Calculation				
λ_q (cm)	Gain (db)	M^2	M^2Y_o ($(ohm)^{-1} \times 10^3$)	f_p (mc)
21.8	13.1	0.552	1.13	744

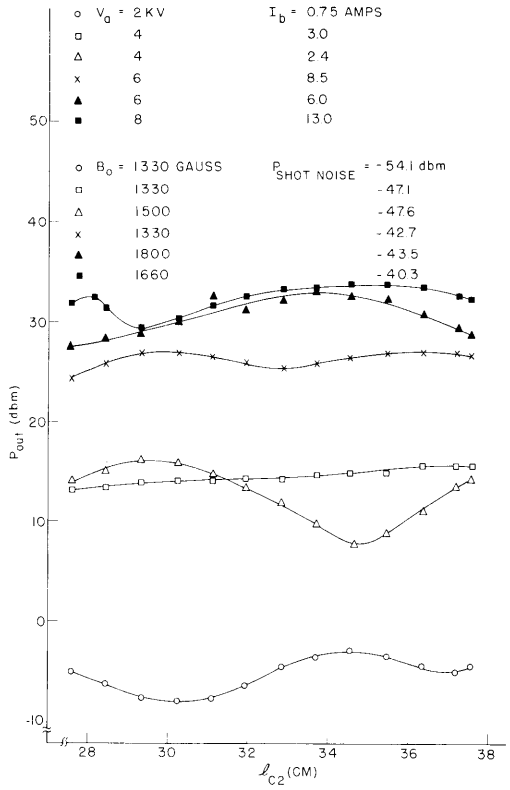

Fig. V-12. Second-cavity noise power output vs distance between cathode and cavity gap for the conical-cathode gun.

Note that the design parameters (V_a = 10 kv, K = 10 microperv, B_o = 1000 gauss) were not achieved. In fact, the gun gave much higher perveances than expected.

b. Cavity-Interaction Measurements

Space-charge wavelength and gain measurements were made for V_a = 2 and 4 kv as shown in Fig. V-11. For V_a = 4 kv, the measured and calculated values of λ_q and two-cavity gain are given in Table V-4. Because of the excessive amount of noise generated by the beam and the limited amount of power available at the input (P_{in} = 20 dbm) gain measurements could not be made for higher voltages.

The noise data presented in Fig. V-12 indicate no growth of noise power output along the beam. In fact, for the V_a = 2 and 4 kv cases, noise space-charge standing waves were observed with wavelengths equal to the ones measured with signal input to the first cavity. For both the cylindrical- and conical-cathode guns it was shown that the noise output from the second cavity (f = 1120 mc) had no relation to the noise observed on the collector current which was in the megacycle range.

P. A. Mandics, A. Bers

References

1. A. Poeltinger, High-perveance hollow electron-beam study, Quarterly Progress Report No. 66, Research Laboratory of Electronics, M.I.T., July 15, 1962, pp. 25-29.

2. A. Bers, Kinematic theory of gap interactions for relativistic electron beams, Quarterly Progress Report No. 66, Research Laboratory of Electronics, M.I.T., July 15, 1962, pp. 29-32.

3. A. Bers, Linear space-charge theory of gap interaction between an electron beam and electromagnetic fields, NTF 221, 53-60 (1961).

4. G. M. Branch and T. G. Mihran, Plasma frequency reduction factors in electron beams, Trans. IRE, Vol. ED-2, No. 2, pp. 3-11, April 1955.

5. A. Bers and A. Poeltinger, High-perveance electron-beam study, Quarterly Progress Report No. 64, Research Laboratory of Electronics, M.I.T., January 15, 1962, pp. 47-48.

6. A. Bers, L. Anderson, and K. Keller, Theory and Design of a Conical Electron Gun for Producing a Hollow Beam, Spencer Laboratory Engineering Report No. PT-277, Raytheon Company, Burlington, Massachusetts, 1962.